Low Temperature Creep of Martensitic Steels under Tensile Loading

M. Münch[1], N. Remalli[1], R. Brandt[1]
[1] University of Siegen, Germany

Contact data
M. Münch, University of Siegen, mathias.muench@uni-siegen.de

Summary
The low temperature creep (LTC) behavior of high strength, quenched and tempered martensitic steels has been investigated. The creep tests are conducted at loads below the yield strength (YS) in a temperature range of 348 K – 423 K. The influence of temperature on LTC is reported and the results are discussed. It has been shown that the materials LTC behavior is well described by a logarithmic law. The temperature dependence of the creep parameter α is discussed in order to find an indication on the LTC mechanism of high strength martensitic steels.

Key Words
Low Temperature Creep, Martensitic Steels, Tensile Loading, Logarithmic Creep, Temperature Dependence, Creep Mechanisms

Introduction
High strength martensitic steels with ultimate tensile strength (UTS) grades beyond 2000 MPa are applied in the powertrain of vehicles owing to their excellent fatigue strength and high creep deformation resistance. However, an increasing demand to downsize combustion engines requires an even higher resistance of steels against LTC. Especially, a superb creep deformation resistance is needed when considering elevated temperatures, e.g. T = 423 K. In general, creep studies are dealing with high temperature creep (HTC) where the considered temperatures are close to the melting temperature T_m of the material, i.e. beyond T > 0.4 T_m. At these high temperatures the creep behavior of alloys and ceramics is well described by a power law. The creep rate controlling mechanism is a thermally activated dislocation glide and climb process. Besides that diffusional flow will appear due to Harper-Dorn and Coble-Creep [1]. In contrast to HTC, LTC at temperatures T < 0.3 T_m seems to be dominated by dislocation glide. However, other mechanisms, e.g. dislocation exhaustion [2] and overcoming of the Peierls-Nabarro stress by the nucleation of double kinks [3], are discussed and considered as well. Although the exact mechanisms of LTC is still unclear, an appropriate phenomenological relationship for the time dependent creep strain $\varepsilon_{cr} = \varepsilon_{cr}(t)$ of high strength steels is revealed according to Oehlert and Atrens [4] and Kassner [5] by

$$\varepsilon_{cr}(t) = \varepsilon(t) - \varepsilon_0 = \alpha * ln(\beta * t + 1). \quad (1)$$

Here, $\varepsilon(t)$ denotes the total engineering strain, ε_0 is the initial strain at t = 0 s after loading (see Figure 1), and α as well as β are material specific creep parameters.

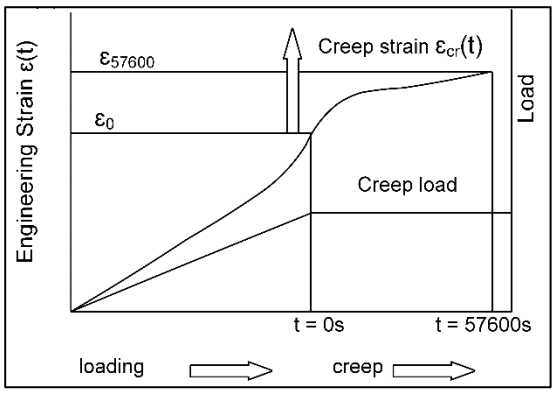

Figure 1: Schematic representation of the loading process [4]

Material and Experiments

The two standard spring steels SAE 9254 and SAE 9260 serve as materials for the LTC tests of this study. Table 1 shows the chemical composition of both steels. The hot rolled wires were shaved, recrystallized and cold drawn to a diameter of 3.7 mm. A fine grained martensitic structure has been setup by an inductive quenching and tempering (QT) process.

Alloys	C	Si	Mn	Cr	P	S	Cu	Al
SAE 9254	0.57	1.39	0.71	0.67	0.017	0.010	0.02	0.002
SAE 9260	0.61	1.90	0.87	0.06	0.018	0.008	0.01	0.002

Table 1: Chemical composition of the spring steels SAE 9254 and SAE 9260, wt%

The temperature dependent UTS, YS and Young´s moduli E of the wires have been determined according to DIN EN ISO 6892-1B, -2B by means of a Zwick Z100 at the Zwick GmbH & Co.KG laboratory (see Table 2).

Temperature	UTS [MPa]		YS [MPa]		E [GPa]	
	SAE 9254	SAE 9260	SAE 9254	SAE 9260	SAE 9254	SAE 9260
RT	2279	2274	2116	2161	204	192
348 K	2242	2266	2099	2137	190	186
373 K	2173	2270	1990	2103	190	186
423 K	2169	2282	1836	1946	178	173

Table 2: Temperature dependent mechanical properties of the spring steels

Uniaxial creep tests have been conducted by means of a mechanical dead weight machine with a 3-zones furnace. A stress σ = 1400 MPa has been applied. In contrast to standard tensile test samples, the here considered specimens are directly cut from the wire to a total length of 120 mm, which are mechanically fixed to the tools. The total engineering strain $\varepsilon(t)$ is measured by means of linear strain gauges with a nominal resistance of 120 ohm, which are glued to the surface of the wires. The measuring length of the strain gauges is 1 mm. The loading was released by means of a manual hydraulic cylinder. The experiments have been conducted at temperatures T = 348 K, 373 K and 423 K, respectively.

Results

The creep curves $\varepsilon_{cr}(t)$ of the here considered materials are shown in Figure 2 (a) for a tensile load σ = 1400 MPa at different temperatures. The measured values of $\varepsilon_{cr}(t)$ are fitted according to Eq. (1). The experimental data and the corresponding fits are represented as symbols and lines, respectively. Figure 2 (b) shows the corresponding creep rate $\dot{\varepsilon}_{cr}(t) = \partial\varepsilon_{cr}(t)/\partial t$ as a function of the creep strain. The creep rate $\dot{\varepsilon}_{cr}(t)$ is calculated by means of a linear fit to the experimental data at the considered time t. It is obvious that the measured values correspond well with the fitting lines and the related coefficients of determination r² are documented in Table 3. The decrement of the creep rate $\dot{\varepsilon}_{cr}(t)$ with creep strain $\varepsilon_{cr}(t)$ shows that stationary creep is still not achieved at the end of the test after 16 h. The fitting parameters α and β are listed in Table 3, whereby the creep parameter values of α are of the same magnitude as reported by Oehlert and Atrens for high strength steels [4].

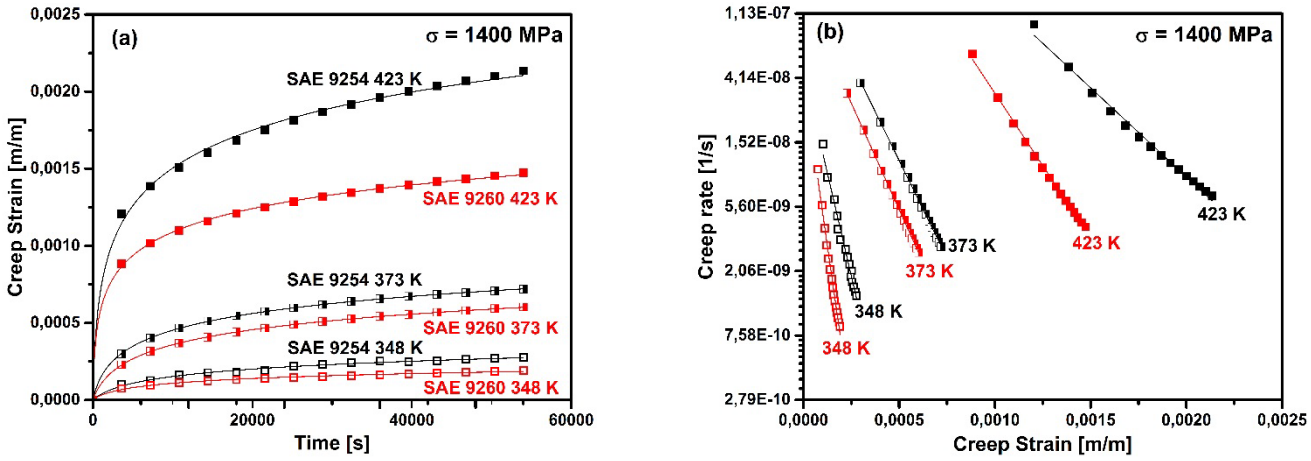

Figure 2: (a) Tensile creep curves and (b) creep rate vs. creep strain curves for a tensile load σ = 1400 MPa at different temperatures

Alloys	T [K]	α [x10^{-4}]	β [x10^{-4} 1/s]	r²
SAE 9254	348	1.79	6.09	0.990
	373	3.78	15.00	0.999
	423	8.27	65.00	0.998
SAE 9260	348	1.10	8.72	0.994
	373	3.48	9.69	0.999
	423	5.09	140.00	0.999

Table 3: Fitting parameters α, β and r² by means of a logarithmic fit for different temperatures T at σ = 1400 MPa

Discussion

The creep curves of the here investigated spring steels correspond well to a logarithmic law. Considering the fits to the experimental data of Figure 2 (b), the creep parameter α represents the inverse of the slope of the fit and β is the intercept of the fitting curve divided by α:

$$ln(\dot{\varepsilon}_{cr}) = \ln(\alpha\beta) - \frac{1}{\alpha}\varepsilon_{cr} \quad \text{with} \quad \alpha = \left[-\frac{\ln(\dot{\varepsilon}_{cr,2}) - \ln(\dot{\varepsilon}_1)}{\varepsilon_{cr,2} - \varepsilon_{cr,1}}\right]^{-1} \quad \text{and} \quad \beta = \frac{\dot{\varepsilon}_{cr,0}}{\alpha}\,. \tag{2}$$

According to Neu [6] both creep parameters are functions of the temperature T and the stress σ. They are defined by,

$$\alpha = \alpha_0 RT\frac{S}{\sigma_e} \quad \text{and} \quad \beta = \beta_0 \exp\left(\frac{-(Q_c - c\sigma_e)}{RT}\right) \tag{3}$$

where R is the universal gas constant, S is the deviatoric stress, σ_e is the equivalent stress, Q_c is the activation energy for LTC, and α_0, β_0 and c are material constants. For uniaxial tensile loading the state of stress is given by

$$\sigma = \begin{bmatrix} \sigma_{11} & 0 & 0 \\ 0 & 0 & 0 \\ 0 & 0 & 0 \end{bmatrix} \tag{4}$$

and the deviatoric stress S is defined as

$$S = \sigma - \sigma_H = \frac{1}{3}\begin{bmatrix} 2 & 0 & 0 \\ 0 & -1 & 0 \\ 0 & 0 & -1 \end{bmatrix}\sigma_{11} \quad \text{with} \quad \sigma_H = \frac{1}{3}\sigma_{11} \tag{5}$$

where σ_H denotes the hydrostatic stress. According to von Mises the equivalent stress σ_e

$$\sigma_e = \sqrt{1/2(\sigma_{11}^2 + \sigma_{11}^2)} = \sigma_{11}. \tag{6}$$

The ratio between the deviatoric stress component S_{11} and equivalent stress σ_e is then a constant value of $2/3$. The partial derivatives of α (see Eq. (3)) with respect to temperature and stress become

$$\frac{\partial\alpha}{\partial T} = \alpha_0 R\frac{S}{\sigma_e} = \frac{2}{3}R\alpha_0 \quad \text{and} \quad \frac{\partial\alpha}{\partial\sigma_{11}} = 0. \tag{7}$$

The temperature dependency of the creep parameter α is shown in Figure 3. The slope of the linear fits represent $\partial\alpha/\partial T$ and yields the value of α_0 (see Eq. (7)). These material constant values of α_0 are $\alpha_0^{SAE\ 9254} = 1.572 * 10^{-6}$ mol/J and $\alpha_0^{SAE\ 9260} = 0.905 * 10^{-6}$ mol/J.

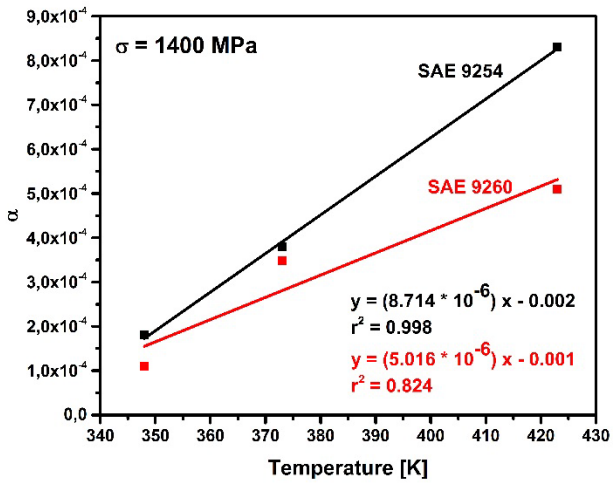

Figure 3: Temperature dependence of creep parameter α for tensile loading at 1400 MPa and different temperatures

The material constant α_0 can be considered as a measure for the creep resistance of the material. According to Eq. (2) and (3) the creep rate reads for times $t \gg \alpha/\dot{\varepsilon}_{cr,0}$

$$\dot{\varepsilon}_{cr} \approx \frac{\alpha}{t} = \alpha_0 * \frac{2RT}{3t}, \tag{8}$$

i.e. the creep rate becomes proportional to α_0. The creep resistance of a material, defined here by the inverse creep rate, is high for small values of α_0.

According to Kassner [5] the creep parameter α is defined by

$$\alpha = \frac{kT}{hv}. \tag{9}$$

Here, k is the Boltzmann constant, h is the strain-hardening coefficient, and v is the activation volume. Then the activation volume v reads with the above considerations

$$v = \frac{kT}{h\alpha} = \frac{3k}{2h\alpha_0 R} = \frac{3}{2Nh\alpha_0} \tag{10}$$

where N the Avogadro constant value is $N = 6.022 * 10^{23}\ mol^{-1}$. The strain hardening coefficient h is approximately given according to Gottstein [9] by

$$h = \frac{d\tau}{d\gamma} \cong \frac{G}{300} \tag{11}$$

The temperature dependent shear modulus G can be obtained from Young´s modulus E (see Table 2) and the Poisson's ratio $\vartheta = 0.29$ for martensitic steels by

$$G = \frac{E}{2(1+\vartheta)}. \tag{12}$$

The activation volumes $v(T)$ of both materials at the considered temperatures are determined according to Eq. (10) and the values are listed below (see Table 4).

Temperature / Material	Activation volume v [x 10^{-25} m^3] SAE 9254	SAE 9260
348 K	1.09	1.81
373 K	0.55	0.61
423 K	0.30	0.51

Table 4: Activation volume values of the investigated materials at different temperatures.

The activation volumes v seems to decrease with increasing temperatures for both materials. It is obvious that the activation volume of SAE 9260 is larger than that of SAE 9254 at each considered temperature. Furthermore, Figure 2 (b) shows that SAE 9260 has a higher creep resistance than SAE 9254 at each considered temperature. Thus, the higher the activation volume v, the higher will be the creep resistance which is in line with Eq. (10) becoming with the creep resistance $\dot{\varepsilon}_{cr}^{-1}$ for times $t \gg \alpha/\dot{\varepsilon}_{cr,0}$

$$v \approx \frac{RT}{Nht} * \frac{1}{\dot{\varepsilon}_{cr}} . \tag{13}$$

Conrad [8] suggest that the possible creep mechanisms are linked to the activation volume $v \approx b^3$. The most likely Burgers vector b in martensitic steels is a/2 [111]. Here, a is the lattice constant, equal to 0.2869 nm. Then, the determined activation volumes for both materials are in the range of $2 * 10^3 b^3 - 1.1 * 10^4 b^3$ in terms of the Burgers vector b. Based on Conrad´s theory of the activation volume, these typical values suggest that intersection of dislocations or non-conservative motion of jogs would be the possible creep mechanisms. Since the activation volume v is defined by the Burgers vector b and the free dislocation line length l_f [9]

$$v = b^2 * l_f, \tag{14}$$

the free dislocation line length l_f of both materials then reads $4.96 * 10^{-7} m < l_f < 2.73 * 10^{-6} m$. Considering the interaction of dislocations as a possible creep mechanism, the forest dislocation density ρ_f is related to the dislocation line length l_f according to [9] by

$$\rho_f = \frac{1}{l_f^2} . \tag{15}$$

The forest dislocation density then reads $1.3 * 10^{11} m^{-2} < \rho_f < 4.0 * 10^{12} m^{-2}$. Since the dislocation densities ρ of martensitic spring steels is much higher $10^{14} m^{-2} < \rho < 10^{16} m^{-2}$ according to Kuno [10], it is unlikely that the intersection of dislocations is the rate controlling mechanism of LTC in the here investigated steels. For this reason the non-conservative motion of jogs remains as the rate controlling mechanism for LTC by Conrad.

Conclusion

The creep behavior of both alloys SAE 9254 and SAE 9260 follows a logarithmic law under tensile loading. By fitting of the creep curves the temperature dependence of the creep parameter α was revealed. It is assumed that the better creep resistance of the alloy SAE 9260 is due to the higher Si content. Considering the magnitude of the activation volume, intersection of dislocations or non-conservative motion of jogs would be the possible creep mechanism. Nevertheless, the large activation volumes leading to relatively long free dislocation lengths l_f and low forest dislocation densities ρ_f raise doubts on the conclusion that intersection of dislocations is the rate controlling mechanism for LTC. Thus, only the non-conservative motion of jogs remains as mechanism. However, further investigations, including investigations with the transmission electron microscopy, are required for an in depth understanding of LTC in martensitic spring steels by means of Conrad´s hypothesis.

Abbreviations

LTC	Low Temperature Creep
HTC	High Temperature Creep
UTS	Ultimate Tensile Strength

YS	Yield Strength

Symbols

α	1. Material specific creep parameter
α_0	1. Material constant
β	2. Material specific creep parameter
β_0	2. Material constant
b	Burgers vector
c	3. Material constant
E	Young´s modulus
ε	Total engineering strain
ε_{cr}	Creep strain
$\dot{\varepsilon}_{\mathrm{cr}}$	Creep rate
ε_0	Initial strain
G	Shear modulus
h	Strain-hardening coefficient
k	Boltzmann constant
l_f	Free dislocation line length
N	Avogadro constant
v	Activation volume
Q_c	Activation energy
R	Universal gas constant
ρ_f	Forest dislocation density
S	Deviatoric stress
σ_e	Equivalent stress
σ_{H}	Hydrostatic stress
T	Temperature
ϑ	Poisson´s ratio

Acknowledgments

We are grateful to Mubea Motorkomponenten GmbH for providing the high strength steels and funding to carry out these investigations.

References

[1] Frost, H.J.; Ashby, M.F.: Deformation-Mechanism Maps – The Plasticity and Creep of Metals and Ceramics, (1982), P. 10.

[2] Mott, N.F.; Nabarro, F.R.N.: Dislocation Theory and Transient Creep, Physical Society Bristol Conference Report, 1-19 (1948), P. 14.

[3] Lawley, A.: Thermally Activated Processes in the Microplastic Region, Microplasticity, 75-90 (1968), P. 85.

[4] Oehlert, A.; Atrens, A.: Room Temperature Creep of High Strength Steels, Acta metall. mater., Vol. 42, No. 5, 1493-1508 (1994), P. 1497.

[5] Kassner, M.E.; Smith, K.: Low temperature creep plasticity, Journal of Materials Research and Technology, Vol. 3 (3), 280-288 (2014), P. 282.

[6] Neu, R.W.; Sehitoglu, H.: Low-Temperature Creep of a Carburized Steel, Metallurgical Transactions A, Vol. 23A, 2619-2624 (1992), P. 2622.

[7] Garofalo, F.: Fundamentals of Creep and Creep –Rupture in Metals, (1965), P. 69.

[8] Conrad, H.: Thermally Activated Deformation of Metals, Journal of Metals, 582-588 (1964), P. 586.

[9] Gottstein, G.: Physical Foundations of Materials Science, (2004), P. 237.

[10] Kuno, T.; Wakita, M.: Spring having excellent corrosion fatigue strength, Pub. No. US2013/0285299 A, (2013), P.5.